Int. J. Rock Mech. Min. Sci. & Geomech. Abstr. Vol. 30, No. 5, pp. 545–550, 1993
Printed in Great Britain.

0148-9062/93 $6.00 + 0.00

Technical Note

Physical Simulation Tests on Jointed Rock and Strength Prediction

W. ZHU†
Z. LIANG†
J. XU†

INTRODUCTION

Most rock masses encountered in engineering are jointed, with the joint sets generally somewhat regular in orientation and distribution. Therefore, emphasis will be mainly put on rock masses with regularly distributed joints. Because of the complicated mechanical properties of a rock mass, thorough study of the failure mechanism of the mass should be based upon successful physical simulation tests and careful monitoring of tests. The purpose of the research is to find a scientific method to predict the global strength of the rock mass.

PHYSICAL SIMULATION TESTS ON THE JOINTED ROCK MASS

Tests of the basic properties of model material

Mechanical properties of model material should be analogous with that of the rock under consideration. They should not satisfy the principle of analogue but also be similar to the prototype rock mass in the constitutive relation curves. In particular, the material should have the dilatancy property, to which most researchers have not paid enough attention. After drying and testing, the authors obtained a mixture as a model material: sands, barites, white polyvinyl emulsion in a given proportion under pressure.

Many small blocks are piled up with some interfaces among them and stuck together in part to form a block simulating a jointed rock mass.

1. The mechanical properties of the model material and the stuck interface. The sample for uniaxial compressive tests has a size of 5 × 5 × 5 cm, in general with a special gravity of 2.2×10^4 N/m^3. The material made in 1990 has a uniaxial compressive strength of $R_{cm} = 0.87$ MPa, an elastic modulus of $E_m = 170$ MPa and a Poisson's ratio of $\mu = 0.22$. The ratio of σ_0/R_{cm} is 0.58 (σ_0 is the corresponding σ when the volumetric strain rate $\epsilon_v = 0$). This material, like most rocks, behaves with dilatancy strength R_{cm}. From Brazilian tests the tensile strength is 0.11 MPa. The shearing resistance from direct shearing tests is $\tau = 0.32 + \sigma \tan 48°$. The material made in 1991 has parameters of $R_{cm} = 0.44$ MPa, $E_m = 77$ MPa, $C_f = 0.29$ MPa and $\varphi = 43°$. Some parts of the rock mass should be stuck to simulate the action of a rock bridge. The direct shearing tests of the bridges gave a strength very close to that of the material.

2. The shearing of property of the joints. The joints were simulated by the free contacted surface between the blocks. The samples of 1990 have the following stiffness and strength parameters: $K_s = 5$ MPa/cm, $K_n = 75$ MPa/cm, $C_j = 0.01$ MPa, $\varphi_j = 39°$; and for the samples of 1991, $K_s = 1.96$ MPa/cm, $K_n = 49$ MPa/cm, $C_j = 0.01$ MPa, $\varphi_j = 37°$.

Experimental study of the jointed rock mass under the condition of plane strain

In the author's engineering practice, the rock mass surrounding some large hydraulic power stations has two nearly-orthogonal joint sets, each have a persistance rate of 50%. The orderly broken-line pattern of joint sets (Fig. 1) will be first studied herein. The large-scale rock mass model in testing is 100 × 50 × 14 cm in size.

1. The strength of "broken-line pattern" of rock masses. The loading path is to apply σ_1 and σ_2 simultaneously up to a certain value first and keep σ_2 constant, then to increase σ_1 stepwise until the failure of samples occurs. Listed in Table 1 are the ultimate stresses for different σ_2 (σ_z is the compressive stress along the direction perpendicular to the sample plane).

Figure 2 shows the strain–stress curve for $\sigma_2 = 0.31$ MPa, in which $p = 1/3\ (\sigma_1 + \sigma_2 + \sigma_z)$, $q = \{[(\sigma_1 - \sigma_2)^2 + (\sigma_2 - \sigma_z)^2 + (\sigma_z - \sigma_1)^2]/2\}^{1/2}$. A relation of $q = 0.1 + 1.72p$ can be derived from the p and q values in Table 1 according to the Drucker–Prager yield criterion, Fig. 3 shows the strength relation among different cases (for testing in 1990). The shearing strength of the rock mass was obtained as $c = 0.05$ MPa, $\varphi = 42°$.

2. The strength of other patterns of a jointed rock mass. In 1991, the simulating tests were conducted on other rock masses with different joint sets, including: (a) ("≡" shaped single joint set); (b) ("λ" shaped set); and (c) ("T" shaped set). The latter two are double joint sets with a persistance of 50% (Fig. 1a). For simplicity, only those testing results of the "T" pattern joint sets are listed in this paper (Table 1, 1991). The strength

†Institute of Rock & Soil Mechanics, Academia Sinica, Wuhan, Peoples' Republic of China.

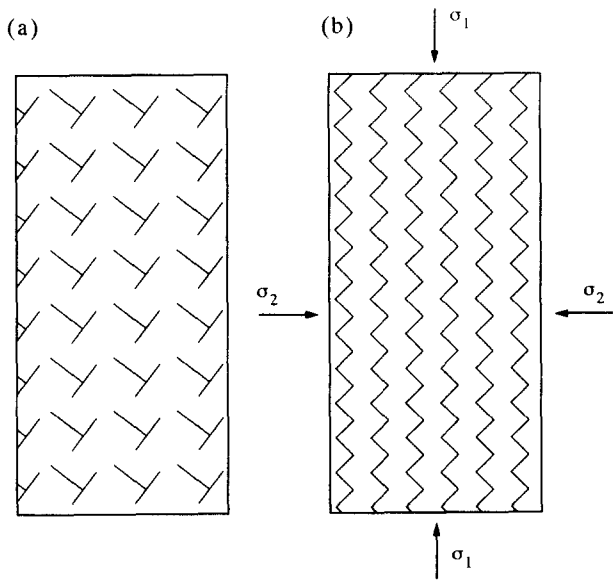

Fig. 1. Patterns of jointed model.

envelope equation can be obtained by fitting the peak values for four different lateral stresses using the least squares method, i.e. $\tau = 0.03 + \sigma \tan 39°$. The corresponding strength relations are shown in Fig. 4.

ANALYSIS OF THE FAILURE MECHANISM OF THE ROCK MASS

The complexity of the failure mechanism of the jointed rock mass makes it difficult to understand. A scientific analysis should be carried out by comprehensive consideration and judgement to predict the rock mass behavior. For this purpose, fracture mechanics and existing results from it should be employed; in addition, stiffness analysis and local stress analysis are also needed.

Stiffness analysis of tested samples

The jointed areas in a rock mass will obviously be weak in stiffness. Take the broken line pattern of joint sets as an example first. The definition of tangential and normal stiffness will be based upon the Goodman joint element analysis. As shown in Fig. 5, a rock mass can

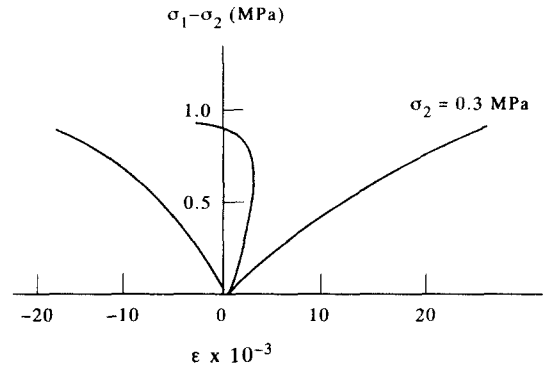

Fig. 2. Stress–strain relation of model.

be considered as two parts, consisting of two different pillars, that is, l_1 with joints and l_2 without joints.

1. Shearing stiffness. If the shearing displacement on a joint surface is $u = \tau/k_s$ with a component of $u_1 = u \cos\beta$ along σ_1 then the strain increment is $\Delta\epsilon_1' = \tau \cos\beta/k_s d_1$. On substitution of the stress state analysis results in the expression for τ, it can be shown that:

$$\Delta\epsilon_1' = \frac{(\sigma_1' - \sigma_2)\sin 2\beta \cos\beta}{2d_1 k_s} \tag{1}$$

2. Normal stiffness. For the same reason, the normal stiffness relation on a joint surface is:

$$v = \sigma/k_s = \tfrac{1}{2}[(\sigma_1' + \sigma_2) - (\sigma_1' - \sigma_2)\cos 2\beta]/k_n$$

and

$$v_1 = v \sin\beta$$

and then

$$\Delta\epsilon_1'' = \frac{v_1}{d_1} = \frac{\sin\beta}{2d_1 k_n}[(\sigma_1' + \sigma_2) - (\sigma_1' - \sigma_2)\cos 2\beta]. \tag{2}$$

The above two additional and the original strain of the simulating material make the total strain:

$$\epsilon_{1j} = \epsilon_{1m} + \Delta\epsilon_1$$
$$= \frac{1}{E}[\sigma_1' - \mu(\sigma_2 + \sigma_3)] + \frac{\sin\beta}{2d_1}\left\{\frac{2}{k_s}(\sigma_1' - \sigma_2)\cos^2\beta + \frac{1}{k_n}[(\sigma_1' + \sigma_2) - (\sigma_1' - \sigma_2)\cos 2\beta]\right\}. \tag{3}$$

It can be seen that the ratio of the effective elastic module E_2 of L_1 to the original E is:

$$E_e/E = \epsilon_{1m}/\epsilon_{1j} = \frac{\frac{1}{E}[\sigma_1' - \mu(\sigma_2 + \sigma_3)]}{\frac{1}{E}[\sigma_1' - \mu(\sigma_2 + \sigma_3)] + \frac{\sin\beta}{2d_1}\left\{\frac{2}{k_s}(\sigma_1' - \sigma_2)\cos^2\beta + \frac{1}{k_s}[(\sigma_1' + \sigma_2) - (\sigma_1' - \sigma_2)\cos 2\beta]\right\}}. \tag{4}$$

Table 1

Sample	σ_1	σ_2	σ_z	p	q	σ_0	σ_0/σ_1
90.1	0.31	0.00	0.02	0.11	0.30	0.19	0.61
90.2	0.62	0.10	0.05	0.26	0.55	0.40	0.65
90.3	0.71	0.15	0.06	0.31	0.61	0.52	0.73
90.4	1.45	0.25	0.23	0.64	1.21	1.25	0.86
90.5	1.28	0.31	0.11	0.57	1.08	1.11	0.87
91.2	0.12	0.01	0.03			0.09	0.73
91.3	0.55	0.09	0.12			0.36	0.66
91.4	0.69	0.14	0.10			0.48	0.70
91.5	0.44	0.05	0.06			0.26	0.60

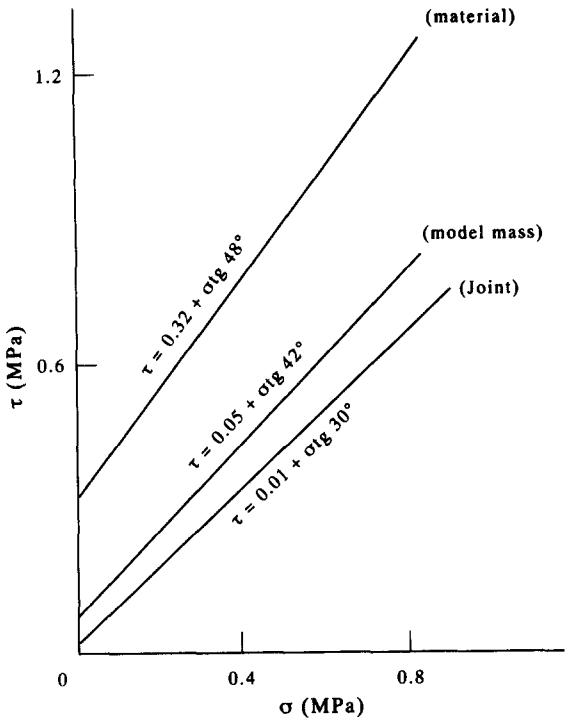

Fig. 3. Strengths for material, joint and model mass.

3. The modified coefficient of stiffness. The rock pillar of L_1 has a smaller stiffness due to the joint sets in it and therefore bears a smaller stress of σ_1'. In contrast to this, the stress of σ_1'' on the L_2 rock pillar is somewhat greater. According to the geometric relation, it can be known that $L_2 = S_1 \cos\beta$ and $L_1 = a \sin\beta$, where S_1 is the rock bridge length of the first joint set, i.e. the length of $\overline{CE}$. From the equalization condition of displacements and strains, the stress ratio is $\sigma_1'/\sigma_1'' = E_e/E$. Because $S_1 = a = 5$ cm and $\beta = 50°$, thus $E_e/E = 0.33$ for uniaxial compression. The real mean normal stress on plane BC is:

$$\sigma_1'' = \frac{\sigma_1(l_1 + l_2)/l_2}{1 + E_e/E} = \eta_2\sigma_1 = 1.50\sigma_1 \tag{5}$$

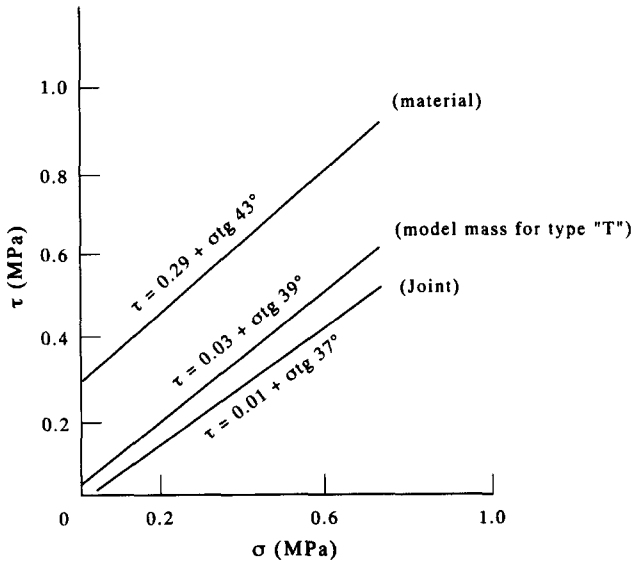

Fig. 4. Strengths for material, joint and model mass.

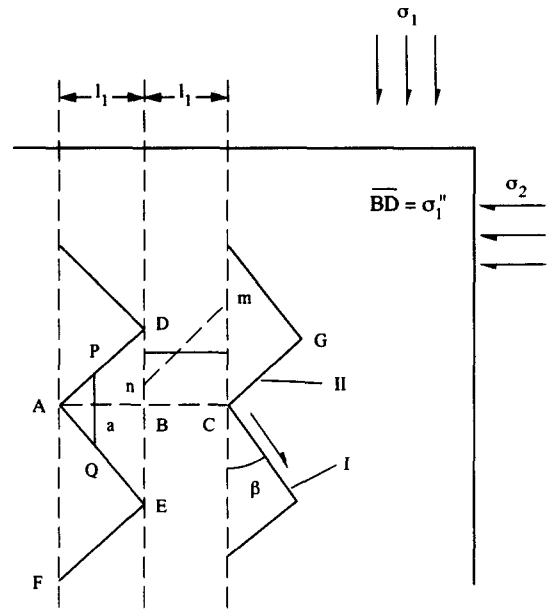

Fig. 5. Stiffness analysis for broken-line joint pattern.

and that on plane AB is:

$$\sigma_1' = \frac{\sigma_1(l_1 + l_2)}{1 + E_e/E} \cdot \frac{E_e}{El_1} = \eta_1\sigma_1 = 0.50\sigma_1, \tag{6}$$

in which

$$\eta_2 = \frac{(l_1 + l_2)}{(1 + E_e/E)l_2}, \quad \eta_1 = \frac{(l_1 + l_2)}{(1 + E_e/E)l_1} \cdot \frac{E_e}{E},$$

which shows a 300% difference between the two stresses. The calculated results for σ_2 ranging from 0.1 to 0.31 give the ratio of $E_e/E = 1/1.27 - 1/2.9$. Therefore, in the case of lateral pressure, E_e/E can be taken as 0.36 approximately, i.e.

$$\sigma_1'' = 1.47\sigma_1, \quad \sigma_1' = 0.53\sigma_1. \tag{7}$$

Fracture mechanic analysis of joints in condition of compression and shearing

In this TN, emphasis will be put on studying the joints of cracks in a compressive stress field; consequently, the stress intensity factor of the cracks with the same strike will be analyzed approximately first. Take the colinear plane cracks as in Fig. 6. The authors, taking into account the friction and cohesion on crack surfaces, derive the contributed force on the surfaces by integrat-

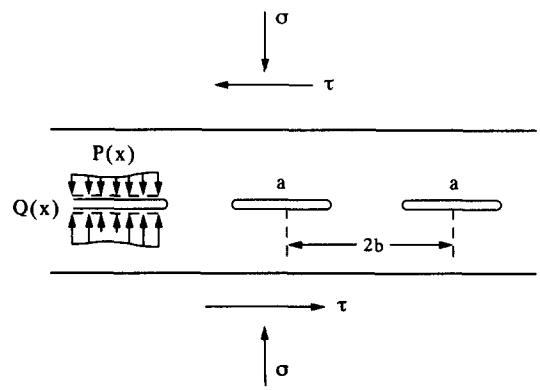

Fig. 6. Stress intensity factor analysis for colinear joints.

integrating the solution for a concentrated force from literature [3], i.e.

$$k_{\mathrm{I}} = \sqrt{2b\tan\left(\frac{\pi a}{4b}\right)}\cdot\sigma + \frac{1}{b}\sqrt{2b\tan\left(\frac{\pi a}{4b}\right)}\int_0^a \frac{p(x)\cos\left(\frac{\pi x}{4b}\right)}{\sqrt{\left(\sin\frac{\pi a}{4b}\right)^2 - \left(\sin\frac{\pi x}{4b}\right)^2}}\,\mathrm{d}x$$

$$k_{\mathrm{II}} = \sqrt{2b\tan\left(\frac{\pi a}{4b}\right)}\cdot\tau - \frac{\tan\psi}{b}\sqrt{2b\tan\left(\frac{\pi a}{4b}\right)}\int_0^a \frac{p(x)\cos\left(\frac{\pi x}{4b}\right)}{\sqrt{\left(\sin\frac{\pi a}{4b}\right)^2 - \left(\sin\frac{\pi x}{4b}\right)^2}}\,\mathrm{d}x - C\sqrt{2b\tan\left(\frac{\pi a}{4b}\right)}.$$

For a compressive stress field, if k_{I} is taken as zero, then the following equation is obtained:

$$k_{\mathrm{II}} = (\tau + \sigma\tan\psi - c)\sqrt{2b\tan\left(\frac{\pi a}{4b}\right)}. \tag{8}$$

Concerning the mutual effects of parallel joints sets, the stress intensity factor can be determined by introducing some modifying coefficients resulting from an analytic or numerical solution. For example, the intensity factor of multi-parallel cracks of the double period, k'_{II} is $k\cdot k_{\mathrm{II}}$ while multiplying (8) by k. The effect of the other joint set intersecting these joints is very complicated. The intensity factor can be determined by using another superposition factor k' or one can be determined by the back analysis method. After remodifying, one can obtain $k'_{\mathrm{II}} = k\cdot k'\cdot k_{\mathrm{II}}$.

If the parameters of k and k' in equation (8) are given because of $\tau = \frac{1}{2}(\sigma_1 - \sigma_2)\sin 2\beta$ and $\sigma = -[\frac{1}{2}(\sigma'_1 + \sigma_2) - \frac{1}{2}(\sigma'_1 - \sigma_2)\cos 2\beta]$ then the modified coefficient is η_1 [see (6) and (7)]. It should be noted here that σ'_1 in (8) is the local normal stress after stiffness modification. In modelling tests for this pattern of joint sets, the related mechanical and geometric parameters are $a = 5$ cm, $\tan\psi = 0.81$, $c = 0.01$ MPa and $b = a$, the measured $k_{\mathrm{IIc}} = 0.73$ MPa/cm$^{1/2}$. While taking $k = k' = 1.2$ and substituting the parameters into the above expressions of k_{II} and k''_{II}, letting $k''_{\mathrm{II}} = k_{\mathrm{IIc}}$ the ultimate fracture stress $\bar{\sigma}_{1s}$ will have the expression (corresponding to the initial compressive and shearing fracture) of:

For different σ_2 value in testing, the corresponding $\bar{\sigma}_{1s}$ can be calculated by substituting the given parameters into (9) (Table 2). It can be seen from Table 2 that as a whole, the stress state is lower than the level at which shearing fracture occurs.

Tensile strain and fracture condition in rock bridge areas

The researchers in their series of tests found, through careful observation of the fracture phenomena occurring at the crack tips and between the cracks, that the compressive fractures took place at rock bridge areas or in the opposite direction to the original crack tip along which a secondary Griffith crack occurred [2, 4, 5]. The rock bridge between the two colinear cracks is the only way of transmitting external loads, so a larger stress concentration will take place at the bridge. If the critical value of the strain is taken as the strength criterion, one can find that a micro-tensile fracture will occur at this area first, which then becomes a larger tensile crack and develops extensively. Reyes [5] and Lemaitre [6] expressed the fracture as such an area by using a damage variable. However, some parameters in this method are difficult to determine. Another method will be proposed in this paper, that is, when the strain at a tensile strain concentration area reaches that corresponding to the measured tensile strength, this creates unstable shearing fracture development and then cuts the rock bridge by shearing failure to form a through failure. What counts is a good knowledge of the influence of stiffness and the

$$\bar{\sigma}_{1s} = \frac{1}{\sin 2\beta - (1-\cos 2\beta)\tan\psi}\left\{\frac{2k_{\mathrm{IIc}}}{k\cdot k'\sqrt{2b\tan\frac{\pi a}{4b}}} + [\sin 2\beta + (1+\cos 2\beta)\tan\psi]\sigma_2 + 2c\right\}$$

$$= \frac{1}{2\sin\beta(\cos\beta - \sin\beta\tan\psi)\tan\psi}\left\{\frac{2k_{\mathrm{IIc}}}{k\cdot k'\sqrt{2b\tan\frac{\pi a}{4b}}} + 2\cos\beta\sin\beta - (\cos\beta\tan\psi)\sigma_2 + 2c\right\} \tag{9}$$

Table 2

Sample	90-1	90-2	90-3	90-4	90-5	Note
σ_2	0.00	1.10	0.15	0.25	0.31	
σ_0	0.19	0.40	0.52	1.25	1.11	Value of inflection point
$\bar{\sigma}_1$	0.31	0.62	0.71	1.45	1.28	Peak value (testing)
$\bar{\sigma}_{1s}$	0.59	1.04	1.24	1.72	1.79	Computed value

Table 3

Sample	90-1	90-2	90-3	90-4	90-5	Note
σ_2	0.00	0.10	0.15	0.25	0.31	
σ_0	0.19	0.40	0.52	1.25	1.11	Testing value
$\bar{\sigma}_1$	0.31	0.62	0.71	1.45	1.28	Peak value (tes.)
$\bar{\sigma}_{1t}$	0.19	0.43	0.57	0.81	1.11	Computing value
$\bar{\sigma}_{1i}$	0.32	0.61	0.76	1.02	1.30	Peak value (com.)

stress concentration extent to obtain a relatively accurate quantitative result.

The ultimate tensile strain of a rock corresponding to its tensile strength can be expressed as $[\epsilon_t] = \sigma_t/E$ (σ_t is the rock's tensile strength). In this case, the strain to be checked near the joint tip at the bridge is:

$$\epsilon_2 = \frac{1}{E}[\sigma_2 - \mu(\sigma_1 + \sigma_3)].$$

Letting this equation equal $[\epsilon_t]$, one can obtain a threshold value of σ_1, σ_1^0, when the macro-tensile failure occurs:

$$\sigma_1^0 = \frac{1}{\mu}(\sigma_2 - \sigma_t) - \sigma_3. \tag{10}$$

As shown in Fig. 5, the stresses on *BC* with a concentration at *C* are not uniformly distributed; nevertheless, their distribution is nearly linear, i.e. shaped like a trapezium (*CmnB*) and, consequently, the area of the trapezium equals that of a rectangle $\sigma_1'' \times BC$, the slope of line *nm* should be linearly dependent on the lateral stress σ_2; that is, the stress concentration factor will reduce with an increment of the lateral stress. In addition, if it is supposed that the normal stress at *C* is $\sigma_1^0 = \text{cm}$, then, according to geometric relations:

$$\sigma_1'' = (f + e\sigma_2)\sigma_1^0$$

By substituting (10) into the equation, one can obtain

$$\sigma_1'' = (f + e\sigma_2)\left[\frac{1}{\mu}(\sigma_2 - \sigma_t) - \sigma_3\right], \tag{11}$$

where parameters f and e can be fitted from testing curves. Based upon the above-mentioned analyses, it is reasonable to suppose that the "knee point" of the volumetric deformation curve of the rock mass corresponds to the critical value of the ultimate tensile strain value [see equation (10)]. Taking stiffness modification and equation (11) into account, one can find

$$\bar{\sigma}_{1t} = \frac{1}{\eta_1}(f + e\sigma_2)\left[\frac{1}{\mu}(\sigma_2 - \sigma_t) - \sigma_3\right], \tag{12}$$

in which

$$\eta_1 = \frac{E}{E + E_e}\left(1 + \frac{a}{s_1}\tan\beta\right).$$

The above equation shows that $\bar{\sigma}_{1t}$ is a critical value. The rock bridge will be seriously weakened due to tensile failure when σ_1 reaches $\bar{\sigma}_{1t}$. Thus, the rock mass will deform under loading to make some joints reach an unstable development point and the joints in the sample will join together rapidly to make the whole rock mass reach an ultimate failure state. Determination of the parameters of f and e by using the values of σ_0 for $\sigma_2 = 0$ and 0.31 from Table 2 gives $d = 0.66$ and $e = 1.06$. For $\sigma_t = 0.11$ MPa and $\mu = 0.22$, the corresponding σ_0 values can be calculated, shown in Table 3, by reference to the σ_2 and σ_3 values in Table 1.

It can be seen from Table 3 that it is reasonable to take $\bar{\sigma}_{1t}$ as an equivalent value of the "knee point" of the sample's volumetric deformation curve. Except for sample 90-4, the results from the rest of the samples are very close to each other.

Based on the above results, $\sigma_0 = \bar{\sigma}_{1t}$ can be considered as the turning point at which the unstable joint development starts, i.e. $\sigma_0 = \bar{\sigma}_{1t}$ is the knee point of the jointed rock mass volumetric deformation. The remaining problems to be studied are to analyze the resistance curve of a joint failure developing and the developing rate. Suppose the developing length of a joint with length a is Δa. When the external load on sample i causes a peak $\bar{\sigma}_{1i}$ of maximum principle stress, the developing rate of a joint can be expressed as $(\Delta\alpha/a)/\Delta\sigma_i$ where $\Delta\sigma_1 = \bar{\sigma}_{ii} - \sigma_{0i}$. The rate is in general related to the lateral stress σ_2.

According to the simulation testing results listed in Table 1, an approximate linear relation can be obtained by substituting the related parameters and fitting it by the least squares method, namely,

$$\frac{\Delta a/a}{\Delta\sigma_i} = -5.16\frac{\sigma_{2i}}{\sigma_{0i}} + 3.92. \tag{13}$$

For a given σ_{2i}, the peak strength of a jointed rock mass, $\bar{\sigma}_{1i}$, can be derived from equations (12) and (13) as follows,

$$\bar{\sigma}_{1i} = \sigma_{0i} + \Delta\sigma_i = \bar{\sigma}_{1ti} + \frac{\Delta a/a}{-5.16\dfrac{\sigma_{2i}}{\sigma_{0i}} + 3.92}. \tag{14}$$

By substituting σ_{it} values for different σ_2 in Table 3 and $\Delta a/a = 2.5/5 = 0.5$ into equation (14), one will obtain various values. The results are also listed in Table 3.

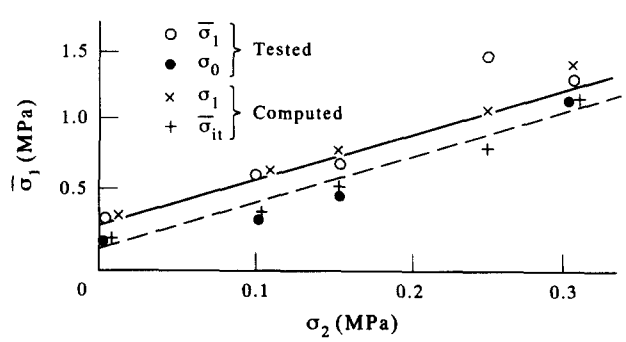

Fig. 7. Comparison of strength values for tested and computed stress levels.

Compared with the peak strengths of the jointed rock mass from tests, most calculated $\bar{\sigma}_{1t}$ values are close to each other, except for Sample 90-4. The above analysis shows that it can be concluded that the method for analyzing and calculating the jointed rock mass strength suggested above is effective. Shown in Fig. 7 are both tested and calculated results for two different stress levels, as well as the fitting curve.

DISCUSSION AND CONCLUSIONS

1. The simulation testing results on the samples with several orderly distributed joint patterns are given. It can be considered that the jointed rock mass strength is lower than the predicted one. The whole friction coefficient is close to the mean value of the rock materials and the joint frictional coefficient when the rock has a joint persistance of 50%; whereas, the cohesion is much more closer to that of the joint.

2. Based upon the stiffness and the local stress concentration analyses, the authors propose an approximate method to calculate the jointed rock mass strength for engineering convenience. The basic assumption of the method is to consider the rock bridge to be damaged mainly caused by the high tensile strain due to stress concentration. As a result, the joint tips are tensilely damaged and even a macro-tensile failure zone will occur to make the joints develop along the compressive and shearing plane, join together and finally cause the whole failure of the rock mass. The method described in this Note is able to deal with the influences of various physical and mechanical parameters of joints and materials, as well as that of the joint geometry distribution.

Acknowledgement—The project was supported by the National Natural Science Foundation of China.

Accepted for publication 8 March 1993.

REFERENCES

1. Zhu W. and Lang Z. Large scale physical simulation tests study on jointed rock mass character. The report of National Natural Science foundation of China (1991).
2. Zhu W., Feng G. and Fang S. The shearing resistance tests study on the model of rock mass with joints in one line (1983).
3. *The Handbook of Stress Intensity Factors* (Edited by Aero-Institute of China). Scientific Press House (1981).
4. Lajtai E. Z. A theoretical and experimental evaluation of the Griffith theory of brittle fracture. *Tectonophysics* **11**, 129–156 (1971).
5. Reyes O. and Einstein H. H. Failure mechanisms of fracture rock—a fracture coalescence model. *Proc. of 7th Int. Congr. of Rock Mechanics*. Vol. II, pp. 333–340 (1991).
6. Lemaitre J. Local approach of fracture. *Engng Fract. Mech.* **25**, 523–537 (1986).
7. Horii H. and Nemat-Nasser Compression-induced microcrack growth in brittle soilds: axial splitting and shear failure. *J. Geophys. Res.* **90**, 3105–3125 (1985).